Supporting Information for "Convective vortices and dust devils detected and characterized by Mars 2020"

R. Hueso [1], C. E. Newman [2], T. del Río-Gaztelurrutia[1], A. Munguira [1], A. Sánchez-Lavega[1], D. Toledo [3], V. Apéstigue [3], I. Arruego [3], A. Vicente-Retortillo [4], G. Martínez [5], M. Lemmon [6], R. Lorenz [7], M. Richardson [2], D. Viudez-Moreiras [5], M. de la Torre-Juarez [8], J. A. Rodríguez-Manfredi [5], L. K. Tamppari [6], N. Murdoch [9], S. Navarro-López [5], J. Gómez-Elvira [5], M. Baker [10], J. Pla-García [5], A. M. Harri [11], M. Hieta [11], M. Genzer [11], J. Polkko [11], I. Jaakonaho [11], T. Makinen [11], A. Stott [7], D. Mimoun [7], B. Chide [12], E. Sebastian [5], D. Banfield [13], and A. Lepinette-Malvite[5]

[1]Física Aplicada, Escuela de Ingeniería de Bilbao, Universidad del País Vasco UPV/EHU, Bilbao, Spain
[2]Aeolis Research, Chandler, AZ, USA
[3]Instituto Nacional de Técnica Aeroespacial (INTA), Madrid, Spain
[4]Centro de Astrobiología (INTA-CSIC), Madrid, Spain
[5]Lunar and Planetary Institute, Houston, TX, USA
[6]Space Science Institute, College Station, TX, USA
[7]Johns Hopkins Applied Physics Laboratory, Laurel, MD, USA
[8]Jet Propulsion Laboratory, California, USA
[9]Institut Supérieur de l'Aéronautique et de l'Espace (ISAE-SUPAERO), Université de Toulouse, Toulouse, France
[10]Smithsonian Institution, Washington, DC, USA
[11]Finnish Meteorological Institute, Helsinki, Finland
[12]Los Alamos National Laboratory, Los Alamos, NM, USA
[13]Cornell Center for Astrophysics and Planetary Science, Cornell University, Ithaca, NY, USA

Contents of this file

1. Supplementary Figures S1 to S8

Additional Supporting Information (Files uploaded separately)

1. Table S1: Catalog of all pressure drops (excel file)
2. Table S2: Catalog of all vortices (excel file)
3. Table S3: Physical characteristics of modeled events (excel file)

0148-0227/22/$9.00

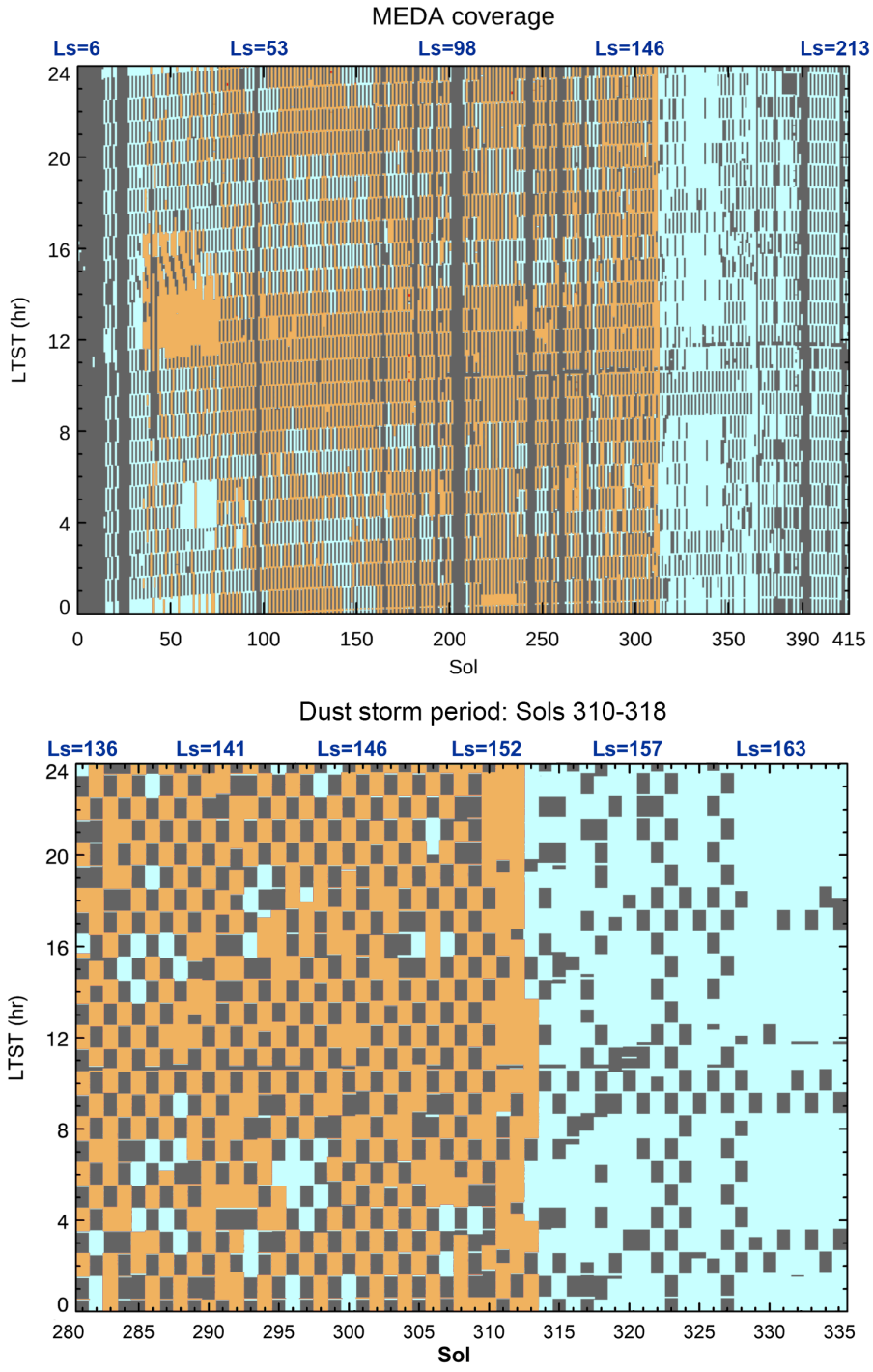

Figure S1. MEDA coverage. Blue indicates times with pressure, RDS and temperature data available. Orange-Yellow indicates times where wind data is also simultaneously available. Grey indicates regions with no MEDA data. Gaps are caused by small hardware problems and science operations constraints. The data follows an odd-even sampling strategy of acquiring continuous data over odd hours on odd sols and continuous data over even hours on even sols. The curved structure in the sampling is produced by operations being performed in Local Mean Solar Time (LMST) and the use of Local True Solar Time (LTST) to display the data. Sols with higher abundance of data correspond to an early investigation of the convective period around sol 50 to prepare the first flights of the Ingenuity helicopter, and a near continuous sampling around sol 340. The bottom panel shows details around a dust storm period (sols 310-318) as discussed in Section 4 in the main manuscript.

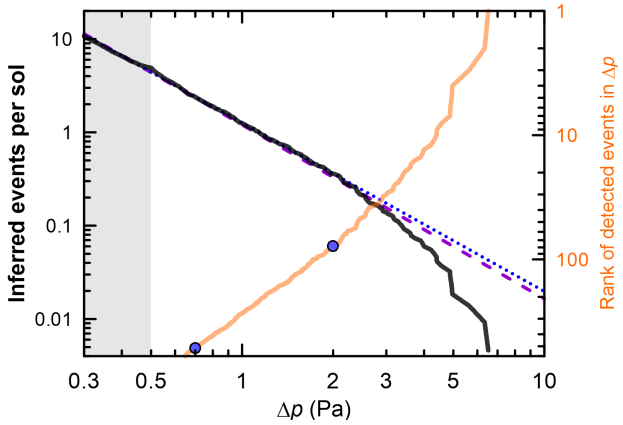

Figure S2. Inferred vortices events per sol and ranking of detected events. The black line (left axis) indicates the inferred number of vortices that pass close enough to MEDA to be detected as a pressure drop. This curve takes into account the normalization by the number of hours observed in each LT period. Dotted-blue line and dashed-purple line show two fits to these data considering either all data (dashed-purple line), or only the frequent and easy to detect events from 0.7 to 2.0 Pa (dotted-blue). The vortices events ranked by the intensity of the detected pressure drop are shown with an orange line (right axis). The two dots show the ranked order of events with pressure drops of 0.7 and 2.0 Pa (520 events stronger than 0.7 Pa and 79 events stronger than 2.0 Pa). Events of these intensities are nearly impossible to miss on the MEDA data and are frequent enough to provide statistics. The power law from these events (dotted-blue) does not differentiate substantially from the power law for all events (dashed-purple). The shaded grey region shows the weak events with pressure dips of 0.3-0.5 Pa where a fraction of them could be missed by our algorithm. Poisson noise dominates the statistics of very large events. There are 13 events more intense than 4 Pa, and only 3 events more intense than 5 Pa.

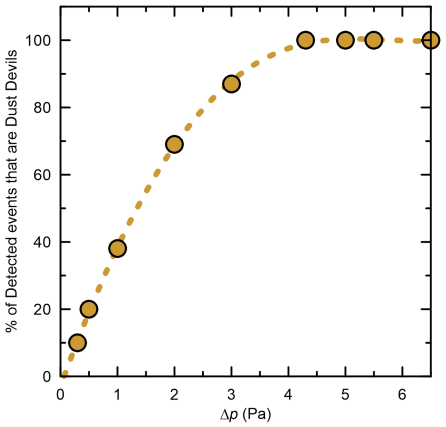

Figure S3. Porcentage of vortices with a pressure drop larger than the values plot on the horizontal axis that are dusty.

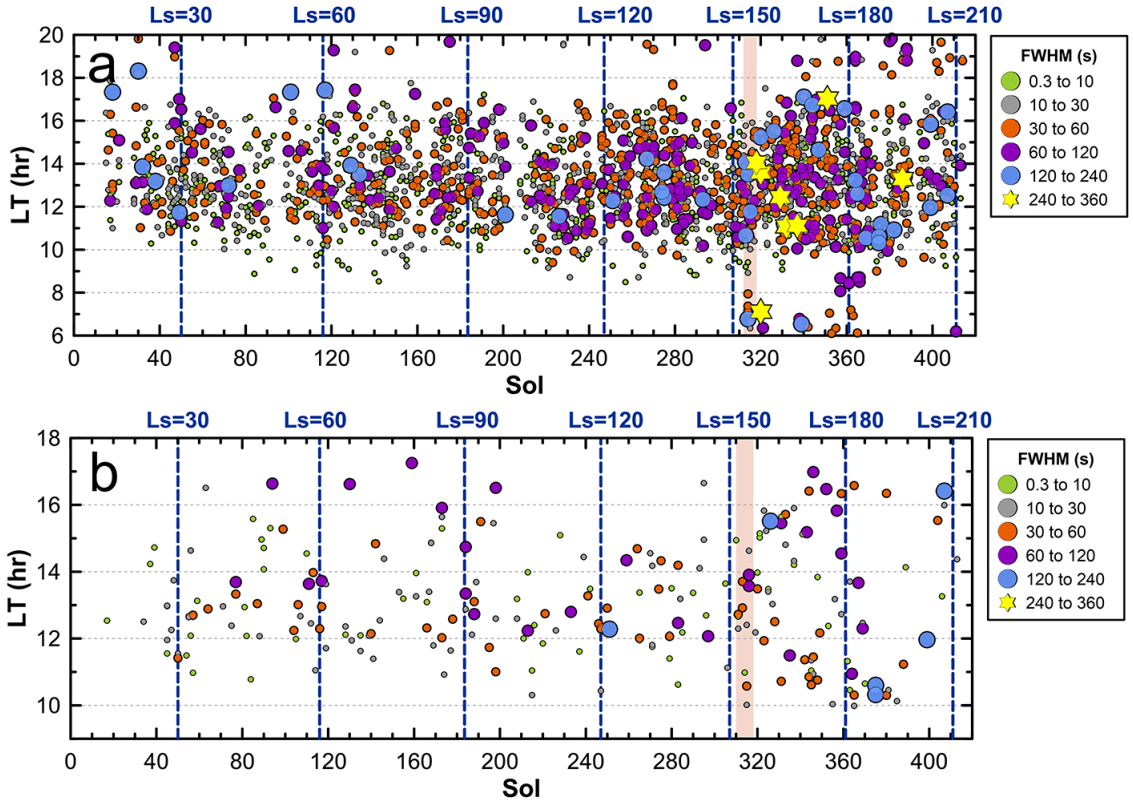

Figure S4. Temporal distribution of vortices (a) and dust devils (b) in terms of the FWHM of the pressure drop. Dust Devils here are considered as vortices with a RDS Top 7 detection of a dip in irradiance of at least 0.5%.

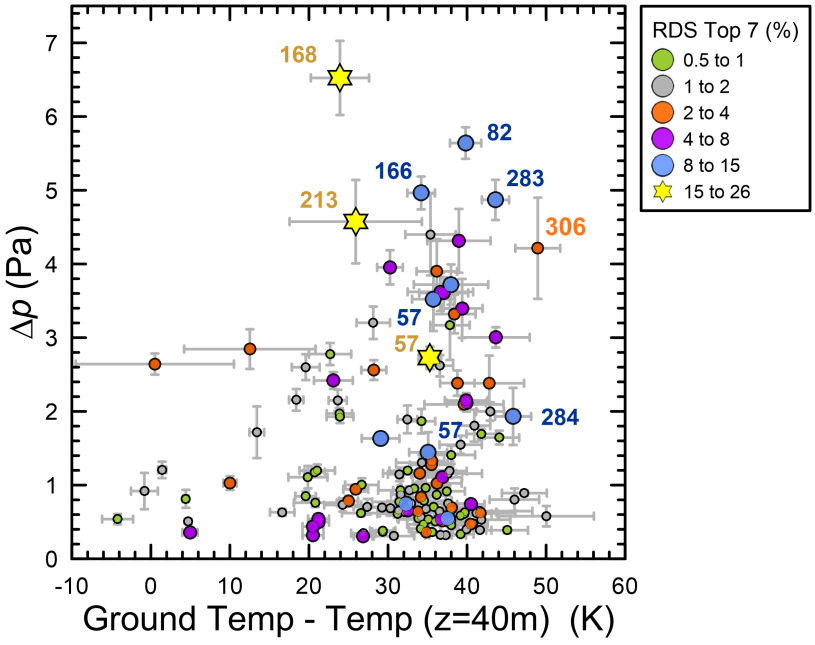

Figure S5. Vortex intensity, thermal gradient and dustiness. Each symbol represents a dust devil where data of the thermal gradient of the atmosphere is known. Horizontal error bars correspond to the standard deviations of temperatures over 8 min, while uncertainties associated to the intensity of the pressure drop is calculated from the deviation of the maximum Δp found and the gaussian and lorenzian fits to the pressure curve of each individual vortex. Numbers indicate sols of particular events. Some of the most intense cases detected are not plot in this figure due to the lack of surface temperatures in some events that occured while the rover was moving.

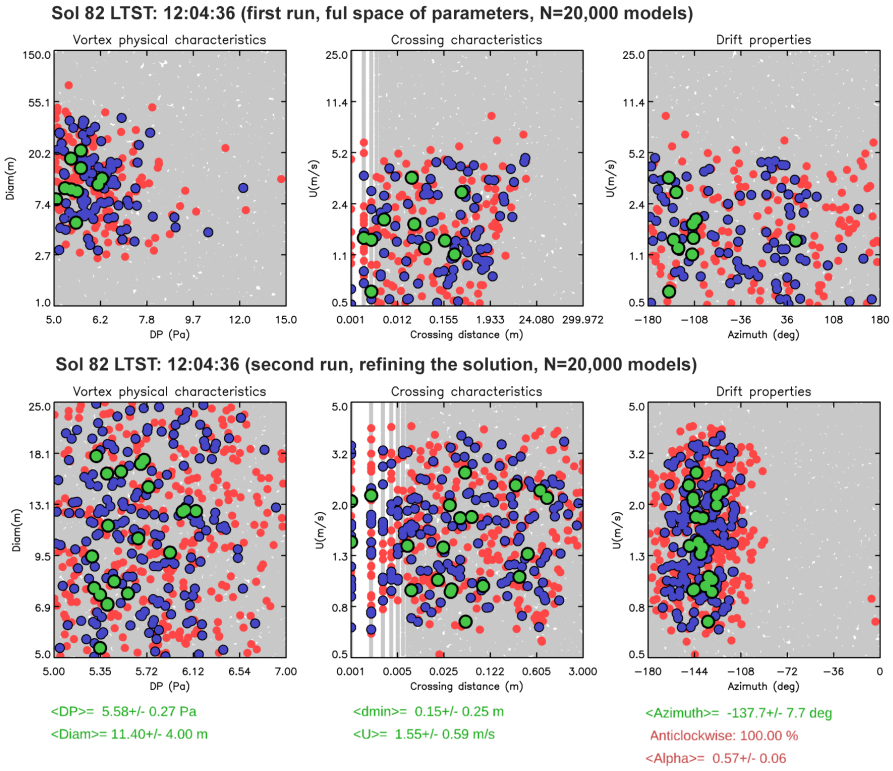

Figure S6. Monte-Carlo analysis of the strong vortex on sol 82. Two runs of 20,000 models (grey dots) are launched first in a wide range of parameters (upper row). The best 10 solutions are shown as green circles, and the best 100 and 200 models are also shown in blue and red to examine possible issues regarding convergence. The statistical analysis of the best 10 models allows to identify a smaller region in the space of parameters where the analysis is repeated extracting the final results from the statistical distribution (lower row).

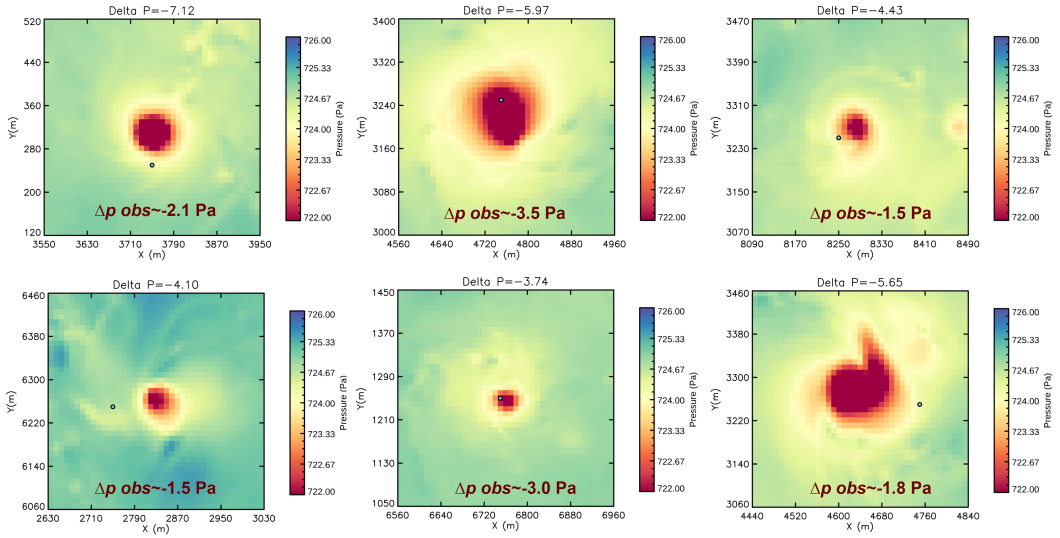

Figure S7. Snapshots of the most intense vortices in the LES at their closest approach to the fixed stations (blue dots). The real pressure drop at the vortex center is compared with the one experienced at the fixed station.

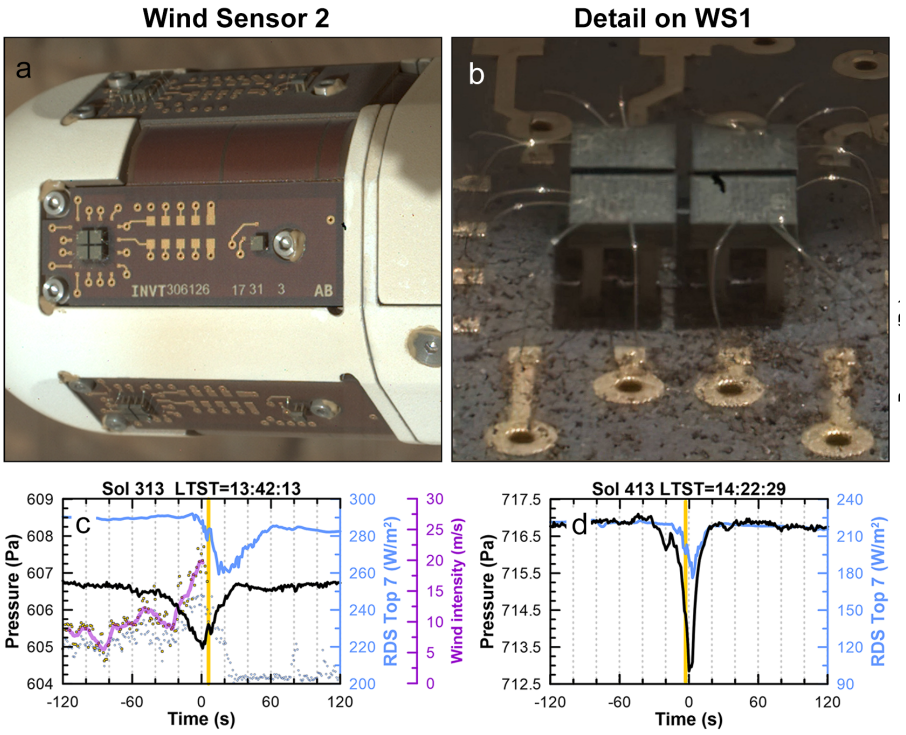

Figure S8. Wind Sensors (a) Image of WS2 on sol 339. (b) Detail of one of the boards of WS1 on sol 339 showing the thin filament possibly damaged in the boards of WS2. (c) MEDA data for the DD on sol 313. Wind data from WS2 was unavailable after the vortex produced its peak pressure drop. Note the shift between pressure and RDS Top 7 data and the failure of WS2 at the time the dust content increases (d) MEDA data for the DD on sol 413. Yellow lines on (c) and (d) indicate the moment when the failure in one of the WS boards occurred.